Concentration Polarization in Reverse Osmosis Membranes: Effect of Membrane Splitting

Andrea P. Reverberi*[a], Bruno Fabiano[b], Cristiano Cerrato[c], Vincenzo G. Dovì [a]

[a] DCCI - Department of Chemistry and Industrial Chemistry, via Dodecaneso 31, 16146 Genova ,Italy
[b] DICCA - Department of Civil, Chemical and Environmental Engineering – Chemical Engineering Section, via Opera Pia 15, 16145 Genova,Italy
[c] DIMSET – Department of Machinery, Energy Systems and Transports, via Montallegro 1, 16145 Genova, Italy
reverb@dichep.unige.it

We propose a simulation study in order to evaluate the effects of concentration polarization damping by splitting a single spiral-wound membrane module in two units connected in series inside the same shell. The reverse osmosis process in each unit is described by the advection-diffusion equation in two dimensions which is solved by a finite difference technique. Several feed regimes and operating conditions are investigated and their influence on the permeate flow rate is assessed for a single and double cell assembly. Finally, optimal operating maps are traced for different configurations of feed flow rate and pressure.

1. Introduction

Reverse osmosis represents a valid technique to separate dissolved salts from solvents and it has found many applications in water desalination (Nair and Kumar, 2013) and in waste treatment (Tagliabue et al., 2014). In the first case, when the permeate phase is the valuable product, reverse osmosis can be considered one of the most important physical process to obtain drinking water for arid countries (Eltawil et al., 2009). In the second one, when the concentrate phase is the useful product, the process aims at obtaining concentrated solutions of polluting and/or radioactive cations and it is one of the most promising technique for radionuclides separation and confinement in nuclear plants (Abdel-Rahman et al., 2011).

Many attempts have been done in order to minimize the effects of fouling and concentration polarization which represent the main causes of impairment in the process yield during time. The paper of Sablani et al. (2001) is an excellent critical review for membrane separation processes and we refer the reader to the references quoted there.

While fouling can be contrasted at a price of adopting upstream operation units in the reverse osmosis plant, concentration polarization is generally considered as a reversible process and its study requires ad-hoc techniques implying an accurate determination of the fluid dynamics and local concentration profiles inside the single cell (Madireddi et al., 1999). The numerical methods are often based on discretization techniques to solve the Navier-Stokes equations in two or three dimensions with finite elements methods, as this approach allows to describe complex geometries of the cells with a good flexibility (Ma et al. 2004). However, finite difference methods may be preferable to finite elements methods in cases of more complicated boundary conditions, or in the presence of discontinuities between initial and boundary conditions (Reverberi et al., 2008).

Ahmad and Lau (2006) investigated the effects of different shapes of spacer filaments in a membrane channel. They proved that unsteady feed regimes and spacer geometries play a very important role to minimize polarization effects. They concluded that the presence of stagnant zones induced by spacers at the membrane surface is a critical phenomenon that triggers concentration polarization. Al-Bastaki and Abbas (1999) proposed a feed regime based on square waves of pressure pulses and they obtained a moderate improvement in the permeate flow rate for sodium chloride solutions in the concentrate phase. Admittedly, this strategy seems to be valid in order to mitigate both concentration polarization and fouling

effects, but limited data have been collected to test the resistance of the membrane to mechanical stresses induced by the pressurization-depressurization cycles for longer times. The functionalization of the inner polymeric membrane structure with inorganic materials (Pascariu at al., 2013) can be adopted in order to make the membrane capable of vibrating when subject to external variable magnetic fields. This effect breaks the concentration polarization layer with an increase in permeate yield.

In spiral-wound reverse osmosis systems, the temperature of the concentrate phase may be used as a control parameter in order to improve the permeate flow rate (Goosen et al., 2002). It was shown that a small temperature increase of only 20 °C may rise the permeate flux by 60 % through a polimeric membrane when the solute is sodium chloride. The cause of this behaviour can be ascribed to a modification in the pore geometries of the membrane and to an increase of the solute diffusion coefficient, whose accurate determination often requires specific estimation techniques (Solisio et al., 2012). In particular, spurious experimental data in inverse problems may give biased diffusivity estimates (Reverberi et al., 2013), owing to secondary effects often related to polymer hydration and interactions between polymer structure and diffusing species.

In this paper, we propose a simulation study where the concentration profiles in a spiral-wound reverse osmosis unit are modelled in two dimensions. The unsteady advection-diffusion equation is solved by a finite difference discretization method. In particular, and this is the core of the work, the membrane inside the single module is splitted in two elements to exploit the mixing effects between membrane units. The paper is organized as follows. Firstly, we describe the model and we give some details about the numerical technique adopted to solve the advection-diffusion equation. Then, we present the results and we compare the process yield in case of membrane splitting with the one corresponding to the unsplitted membrane. In particular, the effects of inlet pressure and fluid speed are investigated according to different membrane geometries and technical solutions. Finally, we draw the conclusions and we trace the direction for future works.

2. The model

The reverse osmosis cell is visualized in Figure 1-a, where a system of orthogonal coordinates is fixed at the centre of the cell inlet for symmetry reasons. In both snapshots (a) and (b), the membranes are represented by lines AB and CD.
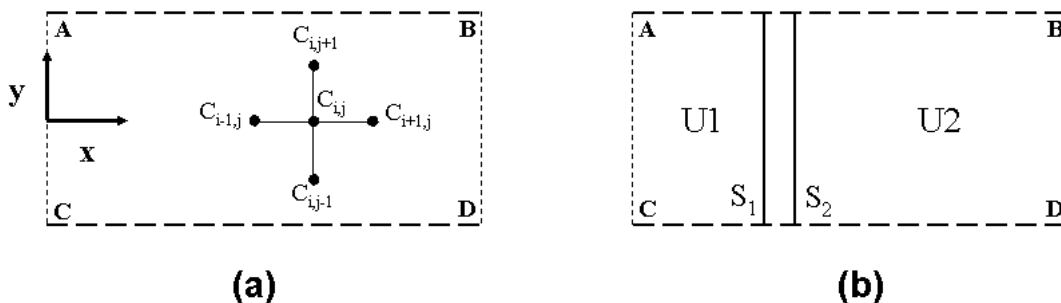

Figure 1: Scheme of membrane channels made of a single unit (a) or a double unit with elements U1 and U2 (b)

The algorithmic scheme adopted in this work was already discussed elsewhere (Cerrato et al., 2009); however it is worth recalling some essential points of it in the following, particularly as far as the boundary conditions are concerned. The dimensionless advection-diffusion equation describing the concentration profile in the membrane channel is:

$$\frac{\partial C}{\partial T} = \frac{\partial}{\partial Y}\left(D_Y\,\frac{\partial C}{\partial Y}\right) + \frac{\partial}{\partial X}\left(D_X\,\frac{\partial C}{\partial X}\right) - U\,\frac{\partial C}{\partial X} - V\,\frac{\partial C}{\partial Y} \tag{1}$$

with

$$C=c/c_0\,,\ X=x/L\,,\ Y=y/h\,,\ T=tu_0/L\,,\ U=u/u_0\,,\ V=vL/u_0h\,;\ D_Y=D_yL/u_0h^2\,;\ D_X=D_x/u_0L \tag{2}$$

where x is the axial coordinate, y is the coordinate normal to the membrane, t is the time, L is the length of the channel, h is the half-height of the channel, u is the axial velocity and v is the velocity normal to the membrane. c_0 is the reference concentration value corresponding to the salinity of the fresh solution

entering the first membrane element, $c(x,y,t)$ is the concentration in the channel, u_0 its velocity at the channel inlet, D_X and D_Y are the axial and radial diffusivities, respectively.

The velocity profiles u and v can be determined by solving the Navier-Stokes equation in the space domain between the membranes. Here, instead, we adopt an alternative method assuming the validity of the semi-empirical velocity expressions proposed by Bhattacharyya et al. (1990) in spiral-wound membranes. With such a choice, U and V are not treated as unknown variables of the problem, but they are a-priori known functions F and G of the space coordinates, namely:

$$U(X,Y) = F\left(X,Y,v_W,\frac{dP}{dX},\eta,u_0\right)$$

$$V(X,Y) = G\left(X,Y,v_W,\eta,u_0\right)$$

(3)

where P is the total pressure, η is the dynamic viscosity and v_W is the fluid velocity normal to the membrane at the membrane surface, defined as wall permeation velocity.

The dimensionless wall permeation velocity $V_w = v_w L/u_0 h$ is related to the membrane permeability A and to the pressure gap ΔP at fixed X between two membrane sides according to:

$$V_W(X,T) = A(\Delta P - \Delta\Pi)L/u_0 h$$

(4)

The transmembrane osmotic pressure $\Delta\Pi$ in Eq(4) depends linearly on the difference between the transmembrane solute concentrations, that is:

$\Delta\Pi = K_0(C_W - C_P)$

(5)

where K_0 is the osmotic pressure constant, C_w is the solute concentration at the wall and C_p is the solute concentration in the permeate phase. Remembering that the rejection factor is defined as:

$R = 1 - C_p/C_w$

(6)

we can eliminate C_p from the previous expression, obtaining:

$\Delta\Pi = K_0 C_W R$

(7)

Figure 1-b represents a scheme of membrane splitting, namely it shows how a single module described in Figure 1-a can be divided into two elements $U1$ and $U2$ where the concentrate phase leaving the first unit at $S_1 = x_1/L$ enters the second one at the dimensionless coordinate $S_2 = x_2/L$. We assume that the concentrate phase coming out of the first unit undergoes a perfect mixing in a narrow space gap between $U1$ and $U2$, whence $S1 \cong S2$. This choice is motivated by the need of finding the upper limit of the permeate flux attainable by splitting the module in two units in series.

The initial conditions for $C(X,Y,T)$, whatever the unit considered, can be written as:

$C(X,Y,0) = 1$

At the channels inlet, we have different boundary conditions for U1 and U2, that is:

$$C(0,Y,T) = 1 \quad \textit{for unit } U1$$

$$C(S_2,Y,T) = \frac{\int_0^1 U(S_1,Y,T)\, C(S_1,Y,T)dY}{\int_0^1 U(S_1,Y,T)dY} \quad \textit{for unit } U2$$

(8)

Analogous considerations must be applied to the velocity field. In fact, the inlet fluid velocity for unit U2 is the average fluid velocity at the exit of U1, namely:

$$U(0,Y,T) = 1 \quad \textit{for unit } U1$$

$$U(S_2,Y,T) = \int_0^1 U(S_1,Y,T)dY \quad \textit{for unit } U2$$

(9)

At the channels outlet, the assumption of null partial derivative may give unphysical results for $U1$ or $U2$. Therefore, it can be assumed:

$$\frac{\partial^2 C}{\partial X^2}(S_1,Y,T) = 0 \quad \textit{for unit } U1$$

$$\frac{\partial^2 C}{\partial X^2}(1,Y,T) = 0 \quad \textit{for unit } U2$$

(10)

The previous conditions ensure the constancy of the first derivative at the exit without enforcing the more restrictive condition of null first derivative, which can be questionable for short membrane channels and even for lengthy channels near the membrane.

On the axis, obvious symmetry considerations lead to:

$$\frac{\partial C}{\partial Y}(X,0,T) = 0 \tag{11}$$

At the membrane surface, the diffusive flux is equal to the convective mass transport through the membrane, that is:

$$D_Y \frac{\partial C}{\partial Y}(X,1,T) = V_W \left(C_W - C_P \right) \tag{12}$$

Replacing Eqs(4,6,7) in the previous equation, we can express the right hand side of Eq(12) as a function of the sole C_w. So, Eq(12) can be used to update the solute concentration at the membrane surface.

At this point, the problem and its boundary conditions have been completely outlined. Different algorithmic choices can be adopted to numerically solve Eq(1); for the present simulations, we adopted a finite-difference scheme with asymmetric expansions of the terms containing the spatial derivatives at the boundaries.

3. Results and discussion

All simulations presented in the following have been realized assuming the values of the geometric and physical constants reported in Table 1.

Table 1: Values of constants adopted in the present simulation

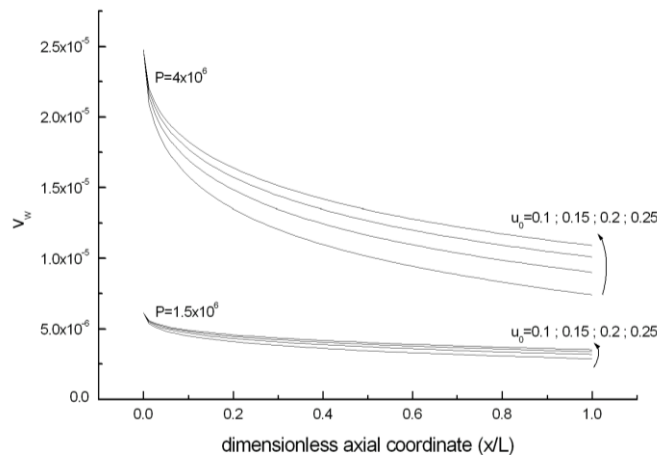| Parameter	Value
Channel length L [m]	2.
Channel height h [m]	$8 \cdot 10^{-4}$
Inlet concentration c_0 [kg m^{-3}]	10.
Rejection factor R	0.98
Diffusion coefficient D_x [m^2 s^{-1}]	$1.61 \cdot 10^{-9}$
Diffusion coefficient D_y [m^2 s^{-1}]	$1.61 \cdot 10^{-9}$
Dynamic viscosity η [kg m^{-1}s^{-1}]	$1 \cdot 10^{-3}$
Osmotic pressure constant K_0 [Pa m^3 kg^{-1}]	$6.89 \cdot 10^4$

Figure 2: Plot of membrane permeation velocity versus the axial coordinate of a single-unit membrane for two values of operating pressures and several inlet velocities

For a single unit membrane, the effects of different feed flows on the permeation velocity are visualized in Figure 2 for two operating pressure values. We remark that, at low pressure, the feed flow regime is nearly uninfluential as far as the polarization is concerned, as all curves for different values of u_0 are nearly horizontal and very close to one another. An opposite situation occurs at higher pressures, where the

permeation velocity decreases markedly for growing values of the axial coordinate of the membrane with a very steep profile at the channel inlet. These aspects will be reconsidered in the case pertaining to the double-unit membrane.
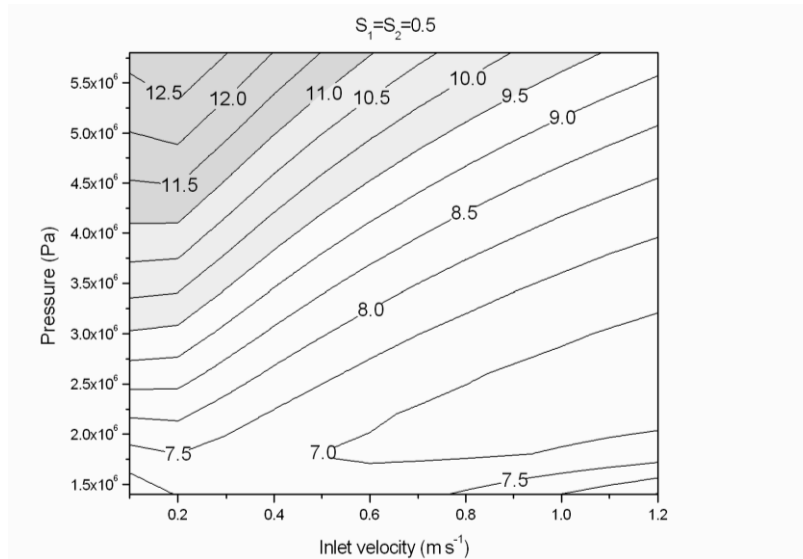

Figure 3: Contour plot of curves at constant G versus the operating pressure and inlet velocity for a double-unit membrane splitted at one half of the total shell length ($S_1=S_2=0.5$)

We define Q_i as the specific permeate flow rate, namely the permeate flow rate per membrane length in the direction normal to the plane *x-y*, obtainable by a configuration with *i* elements. The percent gain in terms of specific permeate flow, obtainable by a double-unit configuration with respect to a single-unit assembly, can be written as $G = 100 \cdot (Q_2-Q_1)/Q_1$.

For a double-unit membrane, the contour lines in Figure 3 are the curves at constant *G* and they are plotted versus the inlet velocity of the first unit *U1* and the operating pressure of the cells. The inlet velocity ranges which the following figure refers to are chosen in a wide interval to have a wide picture of the effects for different operating regimes, typically chosen in commercial applications ($u_0<0.2$ m/s) and in simulation and experimental tests, where u_0 may even exceed 1.0 m/s (Lau et al., 2010). The aforementioned figure refers to a splitting point between membranes located at $S_1=S_2=0.5$. Some interesting aspects should be pointed out, namely:

i) For a wide range of pressure and concentrate flow rates, the gain obtained by a membrane splitting in two units spans over a satisfactory range, often exceeding 10 % of the permeate volume obtainable by a single-unit module.

ii) For the value of *S* here considered, at constant pressures sufficiently higher than the equilibrium value at which $\Delta P=\Delta \Pi$ in Eq (4), the beneficial effects of a membrane splitting decrease for growing inlet concentrate velocity. This result is consistent with the trends of Figure 2 pertaining to the single-unit membrane at high pressure, as the difference $v_w|_{U2,inlet} - v_w|_{U1,outlet}$ decreases for growing values of u_0, thus mitigating the depolarizing role of *U2*.

On the opposite, when $\Delta P \cong \Delta \Pi$, namely at very low pressures, we may have a reverse situation and the gain may increase for growing flow rates. However, this regime is technically meaningless as it corresponds to a minimal permeate flow rate close to its detection threshold.

iii) When the membrane is splitted in two equal elements, that is for $S_1=S_2=0.5$, we observe that the maximum values of *G* are obtained for those values of u_0 typically used in commercial plants, namely $u_0<0.2$ m/s.

4. Conclusions

We have proposed a simulation study of a spiral-wound reverse osmosis cell in order to compare the yield of permeate phase in two different cases of single and double-unit membrane structure assembled in the same shell. We have assumed that the concentrate phase undergoes a perfect mixing before entering the second membrane element. This choice is motivated by the need of finding the upper limit of the aforementioned permeate yield. For some ranges of pressure and concentrate flow rates, the results are

promising and the percent gain in terms of specific permeate flow may be greater than 10 % with respect to the values typical of an unsplitted membrane. As a general trend, the beneficial effects are particularly marked at low channel velocities and high pressures of the concentrate phase. These operating conditions correspond to critical regimes in terms of membrane polarization, as the polarizing effect of a highly concentrated boundary layer at the membrane surface is not damped by the convective effect of the fluid motion. We foresee that the future development of this study will be focused on experimental realizations of staggered membrane coils to assess the validity of such a technique in process optimisation.

References

Abdel-Rahman R.O., Ibrahium H.A., Yung-Tse Hung, 2011, Liquid radioactive wastes treatment: A review, Water, 3(2), 551-565.

Ahmad A.L., Lau K.K., 2006, Impact of different spacer filaments geometries on 2D unsteady hydrodynamics and concentration polarization in spiral wound membrane channel, Journal of Membrane Science, 286(1-2), 77-92.

Al-Bastaki N.M., Abbas A., 1999, Improving the permeate flux by unsteady operation of a RO desalination unit, Desalination, 123(2-3), 173-176.

Bhattacharyya D., Back S.L., Kermode R.I., 1990, Prediction of concentration polarization and flux behavior in reverse osmosis by numerical analysis, Journal of Membrane Science, 48(2-3), 231-262.

Cerrato C., Reverberi A.P., Dovì V.G., Bruzzone A.G., 2009, A switching pressure approach in simulation and optimization of a reverse osmosis unit, Chemical Engineering Transactions, 18, 887-892, DOI: 10.3303/CET0918145

Eltawil M.A., Zhengming Z., Yuan L., 2009, A review of renewable energy technologies integrated with desalination systems, Renewable and Sustainable Energy Reviews, 13(9), 2245-2262.

Goosen M.F.A., Sablani S.S., Al-Maskari S.S., Al-Belushi R.H., Wilf M., 2002, Effect of feed temperature on permeate flux and mass transfer coefficient in spiral-wound reverse osmosis systems, Desalination, 144(1-3), 367-372.

Lau K.K., Abu Bakar M.Z., Ahmad A.L., Murugesan T., 2010, Effect of feed spacer mesh length ratio on unsteady hydrodynamics in 2D spiral wound membrane modules. Industrial and Engineering Chemistry Research, 49(12), 5834-5845.

Ma S., Song L., Ong S.L., Ng W.J., 2004, A 2-D streamline upwind Petrov/Galerkin finite element model for concentration polarization in spiral wound reverse osmosis modules, Journal of Membrane Science, 244(1-2), 129-139.

Madireddi K., Babcock R.B., Levine B., Kim J.H., Stenstrom M.K., 1999, An unsteady-state model to predict concentration polarization in commercial spiral wound membranes, Journal of Membrane Science, 157(1), 13-34.

Nair M., Kumar D., 2013, Water desalination and challenges: The Middle-East perspective: a review, Desalination and Water Treatment, 51(10-12), 2030-2040.

Pascariu V, Avadanei O., Gasner P., Stoica I., Reverberi A.P., Mitoseriu L., 2013, Preparation and characterization of PbTiO3-epoxy resin compositionally graded thick films, Phase Transitions, 86(7), 715-725, DOI: 10.1080/01411594.2012.726727

Reverberi A.P., Bagnerini P., Maga L., Bruzzone A.G., 2008, On the non-linear Maxwell-Cattaneo equation with non-constant diffusivity: shock and discontinuity waves. International Journal of Heat and Mass Transfer, 51(21-22), 5327-5332.

Reverberi A.P., Fabiano B., Dovì V.G., 2013, Use of inverse modelling techniques for the estimation of heat transfer coefficients to fluids in cylindrical conduits, International Communications in Heat and Mass Transfer, 42, 25-31, DOI: 10.1016/j.icheatmasstransfer.2012.12.005

Sablani S.S., Goosen M.F.A., Al-Belushi R., Wilf M., 2001, Concentration polarization in ultrafiltration and reverse osmosis: a critical review, Desalination, 141, 269-289.

Solisio C., Reverberi A.P., Del Borghi A., Dovì V.G., 2012, Inverse estimation of temperature profiles in landfills using heat recovery fluids measurements, Journal of Applied Mathematics, Volume 2012, article number 747410, DOI: 10.1155/2012/747410

Tagliabue M., Reverberi A.P., Bagatin R., 2014, Boron removal from water: needs, challenges and perspectives, Journal of Cleaner Production, DOI: 10.1016/j.jclepro.2013.11.040 (in press).